

Corrosion Behavior of Nitrogen Ion Implanted Stainless Steel

Hee Jae Kim* and R. F. Hochman**

**Department of Weapons Engineering
Korea Military Academy*

***School of Materials Engineering
Georgia Institute of Technology
Atlanta, Georgia 30332*

ABSTRACT

The corrosion behavior of nitrogen ion implanted 440C stainless steel was studied as a practical application of ion implantation. 440C stainless steel was subjected to the same implantation condition which showed the significant improvement of corrosion resistance of a high purity iron. The composition and structure of implanted layer were examined. The corrosion tests of the samples were performed in deaerated 1N H₂SO₄ and 0.1M NaCl aqueous solution using a potentiodynamic polarization method. The corrosion mechanisms of nitrogen ion implanted 440C stainless steel were investigated.

1. INTRODUCTION

The use of ion implantation as an effective means for changing the surface properties of materials has a considerable interest in the past decade. Although other properties such as tribological properties may be equally or more important for a particular application, protection against corrosion by ion implantation comes to be considered [1,2]. There are a number of unique aspects of corrosion in this process which have been only partially investigated. The uniqueness is in the special profile of the concentration as a function of the depth below the surface and in the possibility of producing distributions of elements regardless of the

solubility of the system unattainable by conventional metallurgical technique. In the previous work [3], the authors studied the corrosion behavior of nitrogen ion implanted high purity iron as a model system to avoid the complications which alloy additions would introduce. In their study, nitrogen implantation with a fluence of 2.5×10^{17} ions cm⁻² at 100 KeV significantly increased the corrosion resistance of the iron in both acidic and chloride solutions.

The present study extends the experiment of nitrogen ion implantation into iron to 440C stainless steel, which is often used in bearings and cutting implements where superior corro-

sion resistance is required as well as hardness and wear resistance. Nitrogen implantation was expected to beneficially modify the corrosion characteristics of 440C stainless steel similar to that found for the iron [3]. 440C stainless steel was implanted with nitrogen ions with the same implantation condition which had produced the excellent corrosion resistance in iron. The composition and structure of the implanted layer of the steel were examined to evaluate the corrosion characteristics of nitrogen ion implanted steel. The mechanisms by which ion implantation affected the corrosion behavior of the steel were investigated.

2. EXPERIMENTAL PROCEDURES

The substrate material used in this study was AISI 440C stainless steel. The pre-implanted material was heat-treated as follows: (a) austenitized at 1055 °C for one hour, (b) oil-quenched to 50-65.6 °C, (c) tempered for one hour at 163 °C, (d) cooled in air to room temperature, (e) soaked in liquid nitrogen for 30 minutes, and (f) again tempered as in (c) and (d) above. The composition of 440C stainless steel is given in Table 1.

Table 1. Chemical Composition of 440C Stainless Steel (Wt. %).

Fe	C	Cr	Mn	Mo	Si
bal.	0.95-1.20	16-18	< 1.00	< 0.75	< 1.00

Optical micrograph of the pre-implanted 440C stainless steel is shown in Figure 1. The steel has a uniform distribution of small precipitates about 0.5 microns in diameter, constituting approximately 17 percent of the volume fraction (measured by the point counting method [4]) of the alloy.

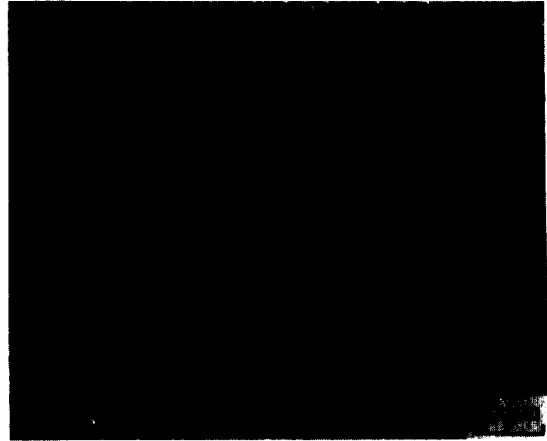


Figure 1. Optical Micrograph of 440C Stainless Steel.

Test specimens were produced by the same process of previous work [3]. Nitrogen ions were implanted with a fluence of 2.5×10^{17} ions cm^{-2} at 100 KeV into the polished surfaces using a commercial ion implanter.

Microstructural and chemical characteristics of the specimen surfaces and sub-surface region were evaluated to characterize the conditions produced by ion implantation and the effect of corrosion testing. Several surface analysis techniques, including Auger electron microscopy (AES), x-ray photoelectron microscopy (XPS or ESCA), transmission electron microscopy (TEM), and scanning electron microscopy (SEM) described in the previous work [3], were employed to characterize the implanted layer and corroded surfaces.

Aqueous corrosion tests were conducted with a single-sweep potentiodynamic polarization technique to characterize the corrosion behavior of implanted surfaces. Polarization experiments were performed in deaerated 1N H_2SO_4 and deaerated 0.1M NaCl aqueous solutions. Deaeration was started two hours prior to testing by bubbling nitrogen gas through

the test solution. The specimen to be analyzed was put into the solution five minutes before testing to reduce pre-reaction with the test solution. The solution was agitated during testing with a magnetic stirrer. All potentials were monitored with respect to a saturated calomel electrode (SCE) at 25 °C. The polarization scan was started 300 mV below the open circuit potential in the noble direction. The scan was then driven in the anodic direction to the transpassive or breakdown potential. Scanning in the cathodic range was attempted to remove or reduce the oxide film during or after implantation. The voltage was scanned at 1 mV sec⁻¹. This high scan rate was used to prevent excessive modification of the surface alloy composition during the experiment.

3. RESULTS AND DISCUSSION

Auger surveys of the unimplanted and post-implanted 440C stainless steel were taken to determine the elements present in the surface region of the samples. Figure 2 show typical Auger surveys of the matrix and a precipitate in 440C stainless steel after argon ion etching to a depth of about 50 Å. The Auger spectrum peaks of the matrix, Figure 2(a), revealed that Fe (80 at. %), Cr (10 at. %), and C (10 at. %) were present. In the precipitate, Figure 2(b), a high concentration of carbon (44 at. %) was observed with Cr (34 at. %) and Fe (22 at. %) indicating that the precipitate is possibly an iron-chromium carbide.

After an Auger survey was taken of the as-implanted surfaces, a depth profile was taken using a sputter rate of about 55 Å per minute as determined with a Ta₂O₅ standard. Figure 3 is a depth profile of the near-surface region of 440C stainless steel implanted with a fluence of 2.5×10^{17} nitrogen ions cm⁻² at 100 KeV.

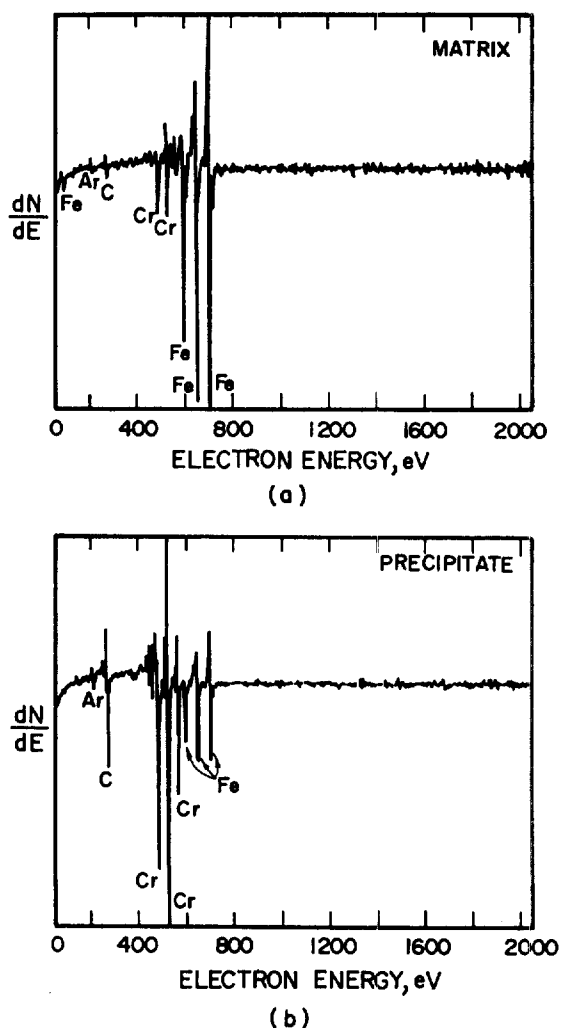


Figure. 2. Auger Electron Spectra Obtained from 440C Stainless Steel After Argon Ion Etching to A Depth of 50 Å
(a) The Matrix and (b) a Carbide Precipitate.

The maximum nitrogen concentration was about 22 at. % and resided about 1000 Å beneath the surface. The total projected range was about 2000 Å. The maximum concentration of implanted nitrogen in 440C stainless steel appeared greater than that found for iron subjected to the same implantation condition [3].

The N 1s and Cr 3p_{3/2} electron spectra

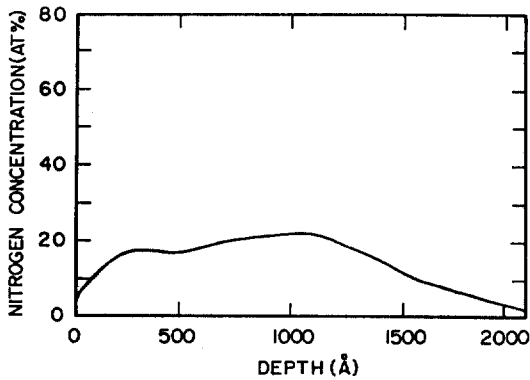


Figure 3. AES Depth Profile of the Near-Surface Region of the Matrix of 440C Stainless Steel Implanted with 2.5×10^{17} Nitrogen Ions cm^{-2} at 100 KeV.

obtained from the nitrogen ion implanted 440C stainless steel are shown in Figure 4. There was a single peak in the N 1s spectrum of as-implanted steel. It may be attributed to an iron nitride [5]. Chromium oxides were related

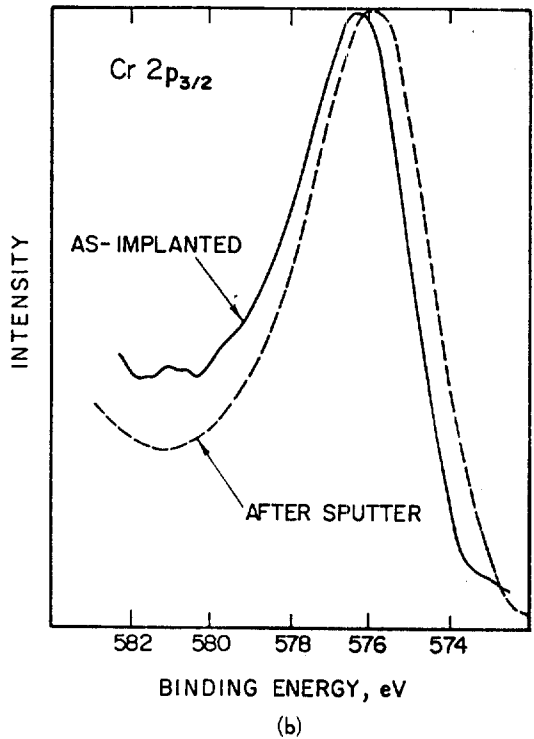
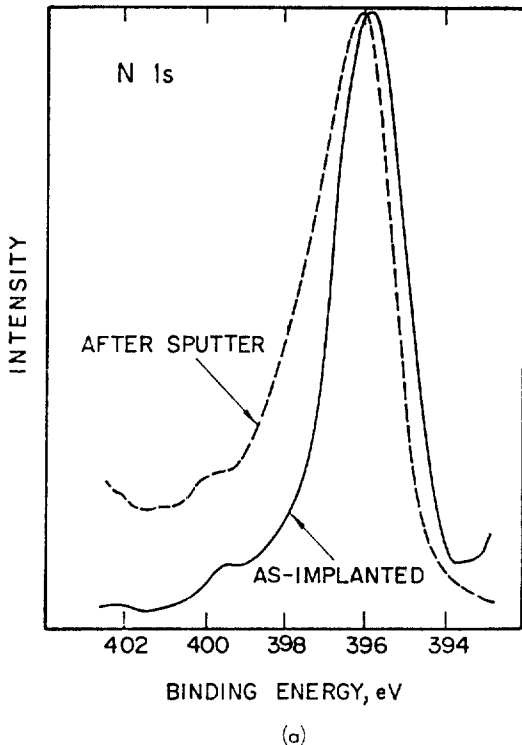


Figure 4. X-ray Photoelectron Spectra of (a) N 1s and (b) Cr $2p_{3/2}$ Electrons in 440C Stainless Steel Implanted with 2.5×10^{17} Nitrogen Ions cm^{-2} at 100 KeV.



to a Cr $2p_{3/2}$ peak in the as-implanted steel with Cr_2O_3 producing a peak at 576.3 eV and CrO_3 at 578.1 eV [6]. After argon ion etching to a depth of 40 Å, the N 1s spectrum had a single peak which could be attributed to the iron nitride [5]. In the Cr $2p_{3/2}$ spectrum, a peak at 575.9 eV due to CrO_2 [6] was observed.

Figure 5 presents the TEM micrograph of tempered 440C stainless steel. The observed structure consisted of a tempered martensite matrix, a large number of spheroidal iron-chromium carbide precipitates, and a small fraction of retained austenite. The substructure of the tempered martensite was composed of heavily tangled dislocations in the martensite lath structure. Retained austenite present is about 5 to 7 volume percent as determined by

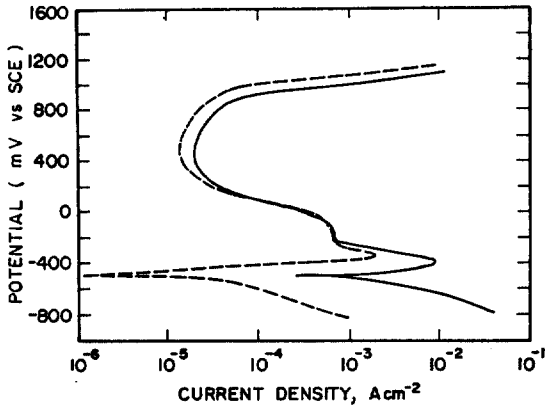
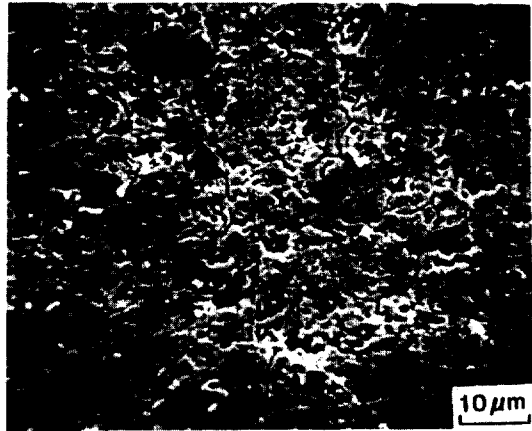


Figure 7. Potentiodynamic Polarization Curves of 440C Stainless Steel Tested in Deaerated 1N H₂SO₄ Solution: Unimplanted (—) and Implanted with 2.5×10^{17} ions cm⁻² at 100 KeV (.....).

nitride with the resultant formation of iron nitride leaving the chromium free in the surface layer.

Figure 7 shows the potentiodynamic polarization curves of unimplanted and implanted 440C stainless steel with a fluence of 2.5×10^{17} nitrogen ions cm⁻² at 100 KeV tested in a deaerated 1N H₂SO₄ aqueous solution. The implanted steel displayed the slightly reduced corrosion rate, critical current density, and passive current density. SEM micrographs of the corroded surface shown in Figure 8 depicted somewhat different forms of corrosive attack.

Figure 9 shows the potentiodynamic polarization curves of unimplanted and nitrogen ion implanted 440C stainless steel tested in a deaerated 0.1M NaCl aqueous solution. Implantation with a fluence of 2.5×10^{17} nitrogen ions cm⁻² at 100 KeV significantly reduced the current densities without pitting in the potential range evaluated. However, the open circuit potential was lowered by 160 mV. Figure 10 shows the SEM micrographs of the corroded surfaces after polarization testing. The implantation produced a surface where pits repassi-



(a)



(b)

Figure 8. SEM Micrographs of 440C Stainless Steel Corroded in Deaerated 1N H₂SO₄ Solution: (a) Unimplanted and (b) Implanted with 2.5×10^{17} ions cm⁻² at 100KeV.

vated and were protected against further pitting in the test, and no developed pits were observed.

The improvement of corrosion resistance of 440C stainless steel by nitrogen ion implantation may be attributed to the same reasons as for iron previously studied [3]. These observations indicate a model parallel to that hypothesized for iron can be used. Nitrogen ion implantation may reduce the crystallographic roughness

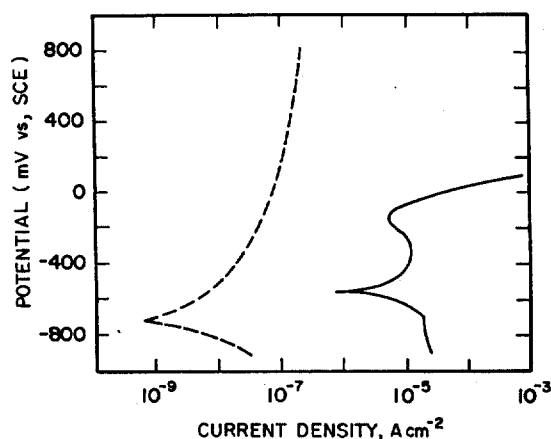


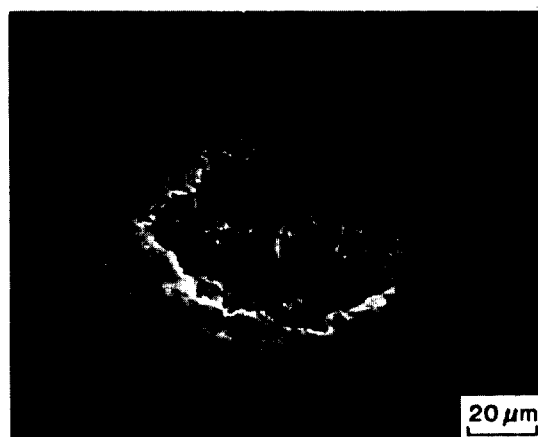
Figure 9. Potentiodynamic Polarization Curves of 440C Stainless Steel Tested in Deaerated 0.1M NaCl Solution: Unimplanted (—) and Implanted with 2.5×10^{17} ions cm^{-2} at 100 KeV (.....).

of steel surface and provide a more homogeneous surface for the formation of a passive film than the crystalline state. This results in the formation of a homogeneous, low stress passive film during corrosion. Significant improved resistance to pitting in 0.1M NaCl solution may be provided by this reason.

Of course, the additional factor of the formation of a Cr rich layer during electrochemical dissolution of the implanted surface may not be disregarded. The enrichment of the surface by the alloying elements such as Cr and implanted ion species during corrosion results in an improved corrosion resistance due to the implanted region acting as a preformed, stable surface layer serving the same function as a passive film.

4. CONCLUSIONS

1. Nitrogen implantation with a fluence of 2.5×10^{17} ions cm^{-2} at 100 KeV into 440C stainless steel produced a high density of tangl-



(a)



(b)

Figure 10. SEM Micrographs of 440C Stainless Steel Corroded in Deaerated 0.1M NaCl Solution: (a) Unimplanted and (b) Implanted with 2.5×10^{17} ions cm^{-2} at 100 KeV.

ed dislocations in the martensite lath.

2. Nitrogen ion implantation into 440C stainless steel increased the corrosion resistance of the steel in a deaerated 1N H_2SO_4 aqueous solution. The implanted steel showed the significant increased pitting resistance in a deaerated 0.1M NaCl aqueous solution. Pits produced in the solution were well-repassivated, and pitting potential was not found in the range tested.

5. REFERENCES

- (1) J.K. Hirvonen, *J. Vac. Sci. Technol.*, **15**(5), 1662 (1978).
- (2) C.R. Clayton, *Nucl. Instr. Meth.*, **182/183**, 865 (1981).
- (3) H.J. Kim and R.F. Hochman, *J. of the Corr. Sci. Soc. of Korea*, **15**(3), 17 (1986).
- (4) J.E. Hilliard and J.W. Cohen, *AIME Trans.*, **221**, 344 (1961).
- (5) I.L. Singer and J.S. Murdy, *J. Vac. Sci. Technol.*, **17**(1), 327 (1980).
- (6) C.D. Wagner, W.M. Riggs, L.E. Davis, J.F. Moulder, and G.E. Muilenberg, *Handbook of X-ray Photoelectron Spectroscopy*, Perkin-Elmer Corp., Eden Prairie, MN (1979), p.72.
- (7) D.H. Jack and K.H. Jack, *Mat. Sci. and Engr.*, **11**, 1 (1973).